PHYSICAL REVIEW B VOLUME 17, NUMBER 3 1 FEBRUARY 1978

Monte Carlo study of the ground state of bosons interacting with Yukawa potentials*

D. Ceperley and G. V. Chester
Laboratory of Atomic and Solid State Physics, Cornell University, Ithaca, New York 14853

M. H. Kalos
Courant Institute of Mathematical Sciences, New York University, New York, New York 10012

(Received 6 July 1977)

We study the ground state of a system of bosons interacting with Yukawa potentials, in both the liquid and solid phases, with a variational and an exact Monte Carlo method. A number of different wave functions to describe the solid phase are investigated. It is found that a Gaussian-Jastrow wave function has a lower energy than either a periodic wave function or a symmetrized Gaussian-Jastrow wave function. We have determined the liquid-solid coexistence curve and discovered that the solid melts when Lindemann's ratio exceeds 0.28. We have also determined that if the solid is superfluid, the superfluid fraction is less than 0.13. A significant conclusion of the comparison of exact and variational results is that the Gaussian-Jastrow wave function for a solid is better than the Jastrow function for liquid when used in a variational calculation. Thus a bias will be introduced when variational calculations are used to estimate crystallization and melting densities. There is a class of Yukawa potentials which do not have a crystalline phase at any density.

I. INTRODUCTION

In recent years, many studies have made of the ground state of liquid and solid helium and several models of neutron matter using the Monte Carlo technique to evaluate the expectation values calculated with a variational wave function.[1] Elsewhere[2] we have reported the results of calculations for a simple model of neutron matter: bosons interacting with a Yukawa potential. We had found that bosons interacting with either the "Bethe",[3] or with the "Chester-Cochran" potential[4] do not crystallize at any density. Because of the relatively low mass, the zero-point motion of the neutrons is too large to localize the neutrons on crystal sites. The calculations in this paper investigate a wider range of Yukawa potentials in order to determine when a crystal forms and the properties of such a crystal.

Consider the ground state of bosons interacting with a Yukawa potential

$$V = \epsilon\sigma \exp(-r/\sigma)r \ . \tag{1}$$

The basic mechanism for crystallization for this potential may be quite different than that of a hard-core system like helium. For hard-core potentials, the system crystallizes at high densities because in that way the particles avoid overlap; it is basically a packing problem. On the other hand, a soft-core potential allows overlap. Indeed, it is likely that the high density phase of any soft-core system is an imperfect gas. The system crystallizes to minimize the total energy, but can do so only if the zero-point motion is small enough.

It might be expected, then, that the ground-state properties of a soft-core system would be quite different from hard-core systems several of which have been extensively studied, both theoretically and experimentally. The Yukawa potential is both soft and short ranged; it does not have the long-range correlations of a coulomb system. A Yukawa crystal may be considerably different from a helium crystal, since the soft core allows exchange effects much more readily.

A Yukawa system is probably a good model for other interactions. For example, it has been used[5] to determine the equation of state of neutron matter with ϵ and σ chosen to reproduce some of the effects of the more complicated Reid potential. For σ equal to infinity the system is the one-component plasma.

The Yukawa potential is convenient from a computational point of view. Since we can simulate at most several hundred particles, the potential must drop off fast enough so that if can be neglected for distances greater than a few interparticle spacings. The alternative is to use Ewald image method of summing over the images of the particles in the periodically extended space. The density in this paper is restricted to the region $\rho^{1/3}\sigma \ll 1$, where the Ewald technique is not necessary, and long-range effects are thought not to be important.

Our paper is organized as follows. In Sec. II we describe the variational and exact Monte Carlo methods which we use to calculate the ground-state energy. With the exception of the treatment of the permanent wave functions these methods have been described elsewhere, and need only be outlined here. We then describe the ground-state calculations for the liquid phase. After that we introduce the four different wave functions for the crystal phase which we have investigated. The usual

Gaussian wave function times a Jastrow function is found to have the lowest variational energy. It should be noted that this is an unsymmetrical function, a symmetrical version of it has a slightly higher energy. Using this wave function, we find both the variational and exact liquid-solid coexistence curve. The remainder of the paper is a discussion of some properties of the ground state, the single-particle density, Lindemann's ratio[6] the existence of vacancies, and an upper bound to the superfluid density in the crystal phase.

II. ASSUMPTIONS AND COMPUTATIONAL METHODS

A quantum system with a Yukawa potential can be characterized by two parameters: the density and an interaction parameter. In this paper we will use reduced units. That is, the unit of length is σ; the reduced density is $\rho\sigma^3$, and energies are in units of $\hbar^2/2m\sigma^2$. The DeBoer "quantumness" parameter measures the kinetic energy relative to the strength of the potential

$$\Lambda^* = h/\sigma\sqrt{m\epsilon} \ . \tag{2}$$

In these reduced units r_s of the electron gas is given by

$$r_s = \rho^{-1/3} 24.49/\Lambda^{*2} \ .$$

The systems which are simulated in this paper contain between 32 and 256 particles placed in a cube with periodic boundary conditions. In several cases, we have increased the size of the system in order to observe the dependence of the energy and other properties on the size of the system. For low densities, that is $\rho \leq 8.0$, 54 particles are generally sufficient.

The methods of calculation are, for the most part, indentical with those outlined in our previous paper of neutron matter.[2] A variational calculation consists in sampling configurations drawn from the trial wave function by the Metropolis random-walk algorithm.[7,8] The variational wave function Ψ_T we have used in this paper has the form

$$\Psi_T = \prod_{j<i} \exp[-u(r_{ij})] \prod_i \theta(r_i) \ , \tag{3}$$

where the pseudopotential $u(r)$ has the same form as the one previously used in neutron matter calculations and found to be a good approximation to the ground state, namely

$$u(r) = A e^{-Br}(1 - e^{-r/D})/r. \tag{4}$$

This pseudopotential is smoothed for large r so that it goes to zero continuously at the edge of the simulation cube.[5] The function $\theta(r_i)$ is used in crystal calculations to localize the particles on lattice sites and is discussed below.

With a given wave function, we evaluate the variational energy as the average of $H\Psi_T(R)/\Psi_T(R)$. The parameters of the wave function are then varied to find the minimum energy. Once the best Jastrow function is found, we calculate other properties of the wave function such as the pressure, two-particle correlation function and the single-particle density matrix.

The method for calculating the exact ground-state energy has also been described elsewhere.[2,9] The basic method is as follows: we begin with points drawn from the variational wave function $\Psi_T^2(R)$. We have found that it is possible[10] to sample the Green's function of the Hamiltonian $\mathcal{H}$

$$\mathcal{H}(\vec{R})G(\vec{R}, \vec{R}') = \delta(\vec{R} - \vec{R}') \ .$$

It is easy to show that if we iterate the equation

$$\Psi_n(\vec{R}) = E \int G(\vec{R}, \vec{R}')\Psi_{n-1}(\vec{R}')\, d\vec{R}' \tag{5}$$

many times Ψ_n will converge to the exact ground state of the system Ψ_o, and the eigenvalue of the equation is proportional to the ground-state energy. In practice, the random walk is importance-sampled with the trial wave function Ψ_T. This means the Green's function actually used is $G(R, R')\Psi_T(R)/\Psi_T(R')$. The result of the iterations will then be $\Psi_o\Psi_T$. Other ground-state properties can be found by a weighted average[11] over the final output configurations. The weights are proportional to $\Psi_o(R)/\Psi_T(R)$ and are calculated by using the importance-sampled Green's function on the final configurations. At the present time, the calculation of the weights can only be done rather crudely; although mathematically the mean value of the weights is given exactly, computationally the variance is quite high. The calculation of the ground-state energy has been done for a variety of problems and proven to be very reliable when the interation for Eq. (5) is carried out 50–100 times.

The results should of course be independent of which trial function ψ_T is used for an importance function in the exact Monte Carlo method. The results displayed in Table VI show that this is nearly always so.

III. LIQUID PHASE

The variational method described above has been used to calculate the liquid energies at 19 different points in the Λ^*, ρ plane. The best Jastrow parameters and the variational energies are given in Table I. When calculations have been carried out for different values of N they are also shown. Our exact calculation are shown in Table II for three of the points in the Yukawa plane. Refer-

TABLE I. Variational results for the liquid phase at several values of $\rho\sigma^3$ and Λ^*. N is the number of particles in the simulation. A, B, and D are the Jastrow parameters (in units of σ), see Eq. (4) of the text. T is the kinetic energy and E the total energy in reduced units ($\hbar^2/2m\sigma^2$).

$\rho\sigma^3$	Λ^*	N	A/σ	$B\sigma$	D/σ	T	E
0.002 44	0.345	54	24.8	0.17	0.19	0.304	0.815 ± 0.008
0.003 66	0.345	32	24.0	0.22	0.18	0.437	1.59 ± 0.02
0.004 88	0.345	54	24.0	0.16	0.18	0.652	2.65 ± 0.01
0.012 2	0.345	54	22.4	0.19	0.19	1.56	11.69 ± 0.02
0.024 4	0.345	108	20.8	0.22	0.18	2.88	34.46 ± 0.07
0.244 1	0.345	54	12.5	0.69	0.11	15.9	730.4 ± 0.4
0.244 1	0.345	128	12.5	0.69	0.11	15.9	729.3 ± 0.4
0.244 1	0.345	250	12.5	0.69	0.11	15.9	729.5 ± 0.3
0.006 10	0.487	54	19.2	0.20	0.4	0.62	2.23 ± 0.01
0.008 84	0.487	54	19.2	0.25	0.4	0.87	4.03 ± 0.01
0.012 21	0.487	108	19.2	0.22	0.3	1.28	6.62 ± 0.04
0.029 8	0.487	54	16.0	0.44	0.3	2.26	24.79 ± 0.05
0.244 1	0.487	128	9.6	1.12	0.2	9.65	373.6 ± 0.2
1.133	0.487	128	6.4	1.56	0.2	31.9	2084.6 ± 0.4
0.029 2	0.539	108	15.2	0.44	0.3	2.11	20.35 ± 0.04
0.069 6	0.536	108	13.1	0.63	0.2	4.18	66.00 ± 0.06
0.244 1	0.539	108	9.9	1.06	0.2	10.4	310.3 ± 0.3
0.488 3	0.536	250	0.75	1.37	0.2	14.5	685.7 ± 0.4
0.029 3	0.629	54	12.8	0.47	0.5	1.67	15.46 ± 0.05
0.069 6	0.629	54	11.2	0.72	0.4	3.16	49.1 ± 0.1
0.244 1	0.629	128	8.8	1.3	0.2	8.09	227.9 ± 0.2

ence 2 contains additional variational and exact results for values of Λ^* appropriate to neutron matter (0.93 and 1.08). Figure 1 shows the radial distribution function computed both variationally and exactly at one density ($\Lambda^* = 0.629$, $\rho = 0.07$). Figure 2 shows the exact structure factor. It is apparent that the exact correlation function has significantly more structure than the variational one. This trend is true for other quantum liquids such as helium.[9,11] Our $S(k)$ is consistent with linear behavior for small k. This suggests that the exact method of computation includes some of the effects of long wavelength phonons.

Using the weights from the exact code we have calculated the single-particle density matrix at one density. (See Refs. 2 and 8 for the method.) It is shown in Figure 3. Its limiting value for large r is the fraction of particles in the zero momentum state, which in this case ($\Lambda^* = 0.629$ and $\rho = 0.07$) is 0.08.

TABLE II. Results of the exact Monte Carlo simulations for three values of $\rho\sigma^3$ and Λ^* in the liquid state. N is the number of particles. T is the "mixed" kinetic energy and F^2 is the square of the pseudoforce.[2] E is the ground-state energy per particle in reduced units (a tail correction has been added). The points correspond to those on Fig. 4.

$\rho\sigma^3$	Λ^*	N	T	F^2	E	Point
0.003 66	0.345	32	0.46	0.42	1.51 ± 0.01	A
0.012 2	0.345	54	1.53	1.54	11.3 ± 0.1	B
0.069 6	0.629	54	3.33	2.91	48.46 ± 0.02	C

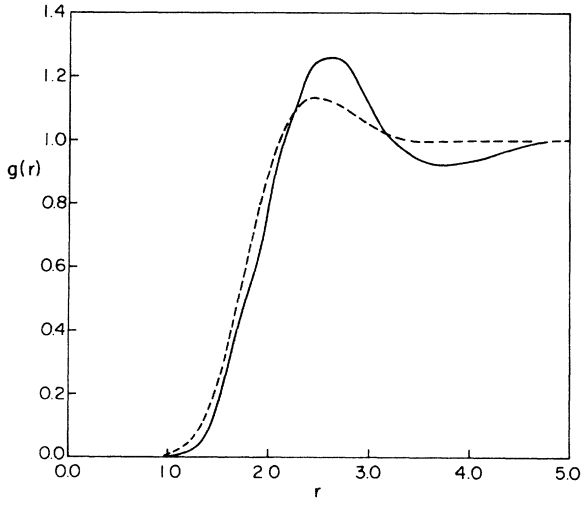

FIG. 1. Radial distribution function $g(r)$ for the liquid at the density $\rho = 0.0696$ and $\Lambda^* = 0.629$. This is the point marked C on Fig. 4. The solid line represents the results of our exact calculations; the variational results are given by the dashed line; r is in reduced units.

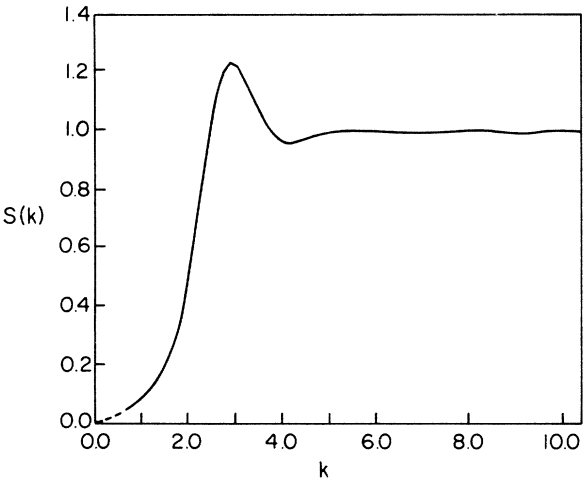

FIG. 2. Exact structure function in the liquid phase. The density and Λ^* are the same as in Fig. 1.

IV. SOLID PHASE

In the solid phase, it is by no means clear what is the optimum wave function. Usually, one multiplies the Jastrow function by a function which has maxima at the crystal lattice sites. We have tried four different forms of the trial function. The first is a harmonic function with no two-particle correlations. The others are products of a Jastrow function with each of the following: a product of Gaussians; a symmetric function with the periodicity of the crystal lattice; and a permanent of Gaussians. The latter yields a symmetric function.

It is probably worthwhile making some general comments on these different types of trial function. Our comments are confined to the last three functions mentioned, all of which contain strong two-particle correlations introduced by the Jastrow factors. Two of the functions are manifestly fully symmetrical, the other (a product of Gaussian localization factors and a Jastrow function) is not. In comparing the results of the unsymmetrical function with the other two, we learn to what degree symmetrizing local functions is important and in particular to what extent exchange takes place in the solid phase. To compare the results obtained from a function which is strictly illegitimate, i.e., unsymmetrical, does provide us with information about the structure of the true ground state. We learn that while there is some exchange it has a small effect on many physical properties, e.g., energy, pressure, and local density, are quite insensitive to symmetrization. When we compare the results obtained from the two fully symmetric functions, we learn something about two entirely different ways of localizing the particles on lattice sites.

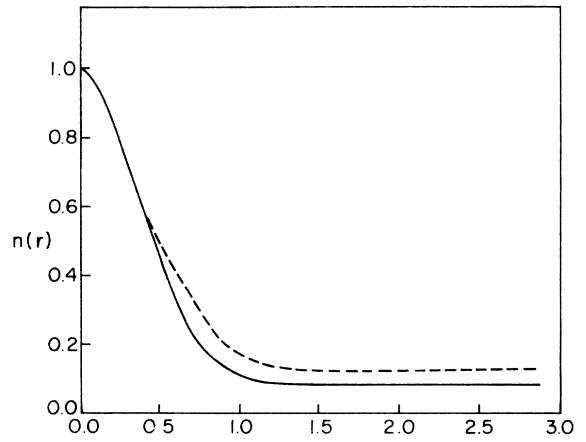

FIG. 3. Single-particle density matrix $n(r)$ in the liquid phase at the same density and Λ^* as Fig. 1. The exact result is the solid curve; the variational result is the dashed curve.

A. Harmonic wave function

The harmonic trial wave function is a product of wave functions centered at the crystal lattice sites; R_i.

$$\psi_h = \exp\left(-\sum_{i=1}^{N} C(\vec{r}_i - \vec{R}_i)^2 \right) . \tag{6}$$

The variational energy of this wave function can be expressed as a sum over the lattice sites:

$$E_h = 3C + \frac{2\pi^2}{\Lambda^{*2}} \sum_i \frac{1}{R_i} \exp(-CR_1^2) \times \left[z\left(\frac{1}{2\sqrt{C}} - R_i\sqrt{C} \right) - z\left(\frac{1}{2\sqrt{C}} + R_i\sqrt{C} \right) \right] , \tag{7}$$

where $z = z(x) = \exp(x^2)\ \mathrm{erfc}\ (x)$, and the summation is over all sites except the one at the origin. The value of the localization parameter C, is adjusted to minimize the energy at $C = C^*$.

A Yukawa crystal is likely to assume either a fcc or a bcc lattice structure, depending on its density. For low density, the close-packed lattice is preferred because the potential drops off exponentially. For high densities, the Yukawa system should go over to the Coulomb, and there the bcc lattice has the lowest energy. Using Eq. (7) it is easy to calculate that in the limit $\Lambda^* \to 0$ the fcc-bcc transition occurs at a density $\rho = 0.196$ with a width $\delta\rho/\rho = 1.2 \times 10^{-5}$. The coexistence curve for finite Λ^* as computed from this wave function is shown in Fig. 4. The transition density

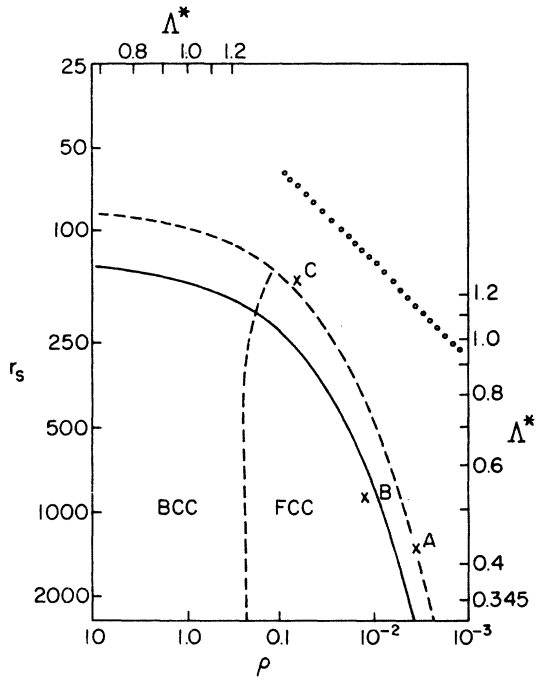

FIG. 4. Phase diagram of Yukawa Bosons. ρ is the reduced density, r_s and Λ^* are measures of the potential defined with Eq. (2). The solid line is the exact liquid-solid coexistence curve; the dashed line is the variational line. The dashed line separating the bcc and fcc solid phases is calculated from the harmonic wave function. The three points marked A, B, and C are points for which we have done exact calculations. The dotted line is the "Bethe" neutron matter potential.[3] The lines of constant Λ^* are parallel to this dotted line.

and width change little with respect to Λ^*. The energies of the two crystal phases are extremely close to each other throughout a wide range of densities. Because of this, it will be very difficult to improve on this determination of the coexistence curve by adding two particle correlations to the trial functions. The difference in energy between the two phases is several orders of magnitude smaller than the Monte Carlo statistical error of the energy. Throughout the remainder of the paper the bcc lattice is used for calculations with $\rho > 0.196$ and the fcc for $\rho < 0.196$.

The harmonic trial function was also used to extrapolate the liquid-solid coexistence curve from the region where we have done exact calculations of the energy to both higher and lower densities. For wave functions of this type, Lindemann's ratio γ is proportional to $C\rho^{-2/3}$. We assume the coexistence curve to lie on a contour of constant $C^*\rho^{-2/3}$. For the density region that we have investigated by variational and exact calculation, the phase boundary does seem to lie on such a contour; the constant γ prescription is therefore probably accurate. The harmonic trial function lacks the important two body correlations and for this reason the Lindemann's ratio as predicted by this model is about $\frac{1}{2}$ of the exact Lindemann's ratio.

B. Gaussian Jastrow wave function

To improve the harmonic wave function one usually introduces two body correlations by multiplying it by a Jastrow wave function. The resulting wave function has been used for variational studies of solid helium[12] and neutron matter.[2,4] The wave function is then

$$\Psi_T = \exp\left(-\sum_i C(\vec{r}_i - \vec{R}_i)^2 - \sum_{i<j} u(r_{ij}) \right) , \qquad (8)$$

where $u(r)$ is given by Eq. (4). This wave function has a much lower energy than the harmonic wave function and over a wide range of densities this wave function has given a lower energy than any other wave function that we have tested. Its chief disadvantage is that it is not symmetric with respect to particle interchange as is the true ground state. The variational energies, optimum Jastrow parameters, and Lindemann's ratio for 19 densities are shown in Table III. Shown in Fig. 4 is the liquid-solid coexistence line predicted from these energies. The line itself is the contour $C^*\rho^{-2/3} = 11.9$ from the harmonic wave function as described in the preceding paragraph. Examination of the phase diagram shows that if Λ^* is larger than 0.60 ± 0.04 this system treated in the harmonic approximation is always in a liquid state; it will not crystallize at any density.

It is difficult to do the double tangent construction on this system because the liquid and solid energies are so close. However one can get an estimate of the transition width from the variational pressures. It is easy to show that in the limit when $\delta\rho/\rho$ is small,

$$\left| \frac{\delta\rho}{\rho} \right| = |P_l - P_s| \Big/ \left[\rho \left(\frac{dP_l}{\delta\rho} \frac{dP_s}{\delta\rho} \right)^{1/2} \right] , \qquad (9)$$

where ρ is the density and P is pressure, calculated in both phases with the use of the virial theorem,

$$P = \tfrac{1}{3}\rho \left(2T + \rho^{\frac{1}{2}} \int dV\, g(\vec{r})\, \vec{r} \cdot \nabla v(r) \right) . \qquad (10)$$

Here T is the kinetic energy per particle, and $v(r)$ is the Yukawa interaction. For the low density liquid-solid transition (to the right of the critical point C on Fig. 3) we obtain $\delta\rho/\rho = 0.01$ for $\Lambda^* = 0.487$ and $\delta\rho/\rho = 0.02$ for $\Lambda^* = 0.345$. These are

TABLE III. Results of the variational Monte Carlo simulation with a Gaussian wave function for various points in the ρ, Λ^* plane. See Table I for the explanation of the symbols. C is the localization parameter of the Gaussians. γ is Lindemann's ratio: rms deviation from the lattice site divided by the nearest-neighbor distance. The systems with $N = 108$ are on a fcc lattice; the others are on a bcc lattice.

$\rho\sigma^3$	Λ^*	N	A/σ	$B\sigma$	$C\sigma^2$	D/σ	T	E	γ
0.002 44	0.345	108	16	0.25	0.078	0.32	0.396	0.87 ± 0.01	0.309
0.003 66	0.345	108	17	0.28	0.12	0.18	0.607	1.64 ± 0.01	0.301
0.004 88	0.345	54	18	0.31	0.20	0.58	0.918	2.54 ± 0.01	0.262
0.012 2	0.345	108	19	0.25	0.39	0.24	2.41	11.2 ± 0.1	0.223
0.024 4	0.345	108	18.4	0.37	0.49	0.17	3.68	33.2 ± 0.1	0.239
0.244	0.345	250	12	0.94	1.95	0.16	19.2	725.8 ± 0.3	0.255
0.244	0.345	256	12	0.94	1.95	0.16	19.2	725.8 ± 0.4	0.254
0.006 10	0.487	54	13.8	0.27	0.16	0.64	0.861	2.32 ± 0.02	0.310
0.008 84	0.487	108	13.6	0.34	0.23	0.56	1.23	4.00 ± 0.02	0.275
0.012 21	0.487	108	12.8	0.31	0.23	0.48	1.46	6.60 ± 0.04	0.325
0.029 8	0.487	54	15.2	0.62	0.58	0.24	3.38	24.39 ± 0.07	0.266
0.244 1	0.487	128	8.8	1.5	2.34	0.16	13.86	371.8 ± 0.3	0.238
1.133	0.487	250	4.8	2.5	4.67	0.08	31.6	2086.4 ± 0.3	0.303
0.029 2	0.539	108	12.8	0.62	0.58	0.32	3.17	20.27 ± 0.04	0.257
0.069 6	0.536	108	11.5	0.91	0.86	0.32	5.35	65.6 ± 0.1	0.269
0.244 1	0.539	108	8	1.6	2.34	0.16	12.7	310.5 ± 0.2	0.256
0.488 3	0.536	250	6.1	2.1	3.5	0.11	19.2	686.2 ± 0.2	0.273
0.029 3	0.629	54	11.2	0.62	0.58	0.48	2.92	15.59 ± 0.04	0.275
0.069 6	0.629	108	9.0	1.0	1.0	0.29	5.0	49.1 ± 0.1	0.260
0.244 1	0.629	128	6.1	2.1	2.34	0.16	10.9	229.1 ± 0.3	0.284

only order of magnitude estimates but they show how close are the densities of the two phases.

C. Periodic wave function

In the Gaussian wave function each particle is localized around a lattice point. With the periodic wave function particles are free to move throughout the lattice, but are subjected to a periodic pseudopotential. The crystal factor of the wave function $\theta(R)$ is chosen to be a product of single-particle terms having the periodicity of the crystal.

$$\theta(R) = \pi_i \theta(r_i) = \exp\left(-\sum_{i=1}^{N} \chi(r_i) \right) , \tag{11}$$

where

$$\chi(r) = \sum_{\vec{k}} C_{\vec{k}} \exp(i \vec{k}_i \cdot r_i) .$$

$\vec{k}$ is a member of the reciprocal lattice and $c_{\vec{k}}$ are additional variational parameters. The complete trial wave function is the product $\psi_J \theta(R)$.

We have previously published[2] calculations with this wave function for neutron matter. Our results were somewhat inconclusive because the system did not crystallize at any density, and in that situation it is not possible to discover the best solid wave function. Lowy and Woo[13] using an approximate integral equation have been able to calculate the phase transition of ^{4}He with this periodic wave function. However, our present Monte Carlo variational calculations show that in all cases where the solid is the preferred phase, the Gaussian-Jastrow wave function has a significantly lower energy than the periodic wave function.

Shown in Table V are the energies, Lindemann's ratio and the number of vacancies at the point B on Fig. 4, corresponding to $\Lambda^* = 0.345$ and $\rho = 0.0122$. Doing a complete search in a large dimensional parameter space of the c_k's with a Monte Carlo program is extremely difficult. The variational calculations for the most part have been done using only one c_k, that having $|k|$ with the smallest nonzero vector in the reciprocal lattice. The last row in Table IV is for a Gaussian-Jastrow wave function. The entry before that is an attempt to reproduce the shape of the Gaussian wave function near the lattice site. This implies that we must choose

$$C_{\vec{k}} = C\rho_0 \int_0^{r_0} d\vec{r}\, (\vec{r}^2 - \vec{r}_0^2) \exp(\vec{k} \cdot \vec{r}) , \tag{12}$$

where $\vec{r}$ is half of the nearest-neighbor distance. Since the energy calculated with this wave function is considerably higher than that of the Gaussian function we must conclude that it is the functional form of the periodic wave function that is at fault, and not merely its shape. In particular, the

Gaussian trial function does not allow double occupancy of lattice sites, while the periodic one does. Let us contrast the Gaussian trial function and the periodic trial function with the same Jastrow parameters. The kinetic energy of the two is nearly the same while the potential energy of the periodic wave function is 0.9 units higher. The percentage of unoccupied Wigner-Seitz cells (V_0) rises from 0.03% to 3.3%. The periodic component of the wave function does nothing to prevent vacancies or double occupancy, and the Jastrow factor in the trial function is not nearly repulsive enough to do so. Our Monte Carlo calculations show that a periodic wave function has a higher energy than the Gaussian wave function for a wide range of densities in the Yukawa crystal. Hence, we believe that this periodic wave function is not a good trial wave function for any crystal with an interparticle potential having a soft ($1/r$) core.

D. Permanent wave function

A completely symmetric function can be constructed from the Gaussian wave function by summing over all permutations (P) of particles to lattice sites. Let $\phi(r)$ be a single-particle orbital about the origin, e.g., $\exp(-Cr^2)$. For a given set of lattice vectors R_i, the permanent wave function is defined as

$$\theta^P = \sum_P \prod_{i=1}^{N} \phi(\vec{r}_i - \vec{R}_{P_i}) . \tag{13}$$

We have sampled the square of this permanent with a generalization of the usual Metropolis[7] Monte Carlo method: the random walk for the permanent trial function is now in both coordinate and permutation space. The probability density to be sampled is

$$F(\vec{R}, \vec{P}) = \psi_T(R)^2 \sum_P \prod_{i=1}^{N} \phi(\vec{r}_i - \vec{R}_{Pi})\, \phi(\vec{r}_i - \vec{R}_i) . \tag{14}$$

The random walk consists of a possible step in coordinate space followed by one in permutation space. The move in coordinate space is chosen in the usual fashion; a new coordinate for one of the particles (say particle i) is chosen inside a cube of side Δ. The probability for accepting this move ($R \to R'$) is

$$q = \min\left(1, \frac{\psi_T(R')^2\, \phi(\vec{r}_i' - \vec{R}_{P_i})\phi(\vec{r}_i' - \vec{R}_i)}{\psi_T(R)^2\, \phi(\vec{r}_i - \vec{R}_{P_i})\phi(\vec{r}_i - \vec{R}_c)}\right) . \tag{15}$$

After the move of particle i, a pair permutation between particle i and all other particles is attempted. That is, for each particle $j \neq i$, a trial permutation $P_t(k)$ is constructed where

$$P_t(k) = \begin{cases} P(j), & k = i \\ P(i), & k = j \\ P(k), & \text{otherwise} . \end{cases} \tag{16}$$

The probability for accepting this permutation is

$$\min\left(1, \frac{\phi(\vec{r}_j - \vec{R}_{Pi})\phi(\vec{r}_i - \vec{R}_{Pj})}{\phi(\vec{r}_j - R_{Pj})\phi(\vec{r}_i - \vec{R}_{Pi})}\right) . \tag{17}$$

Since the majority of permutation exchanges are rejected, this is not the most efficient algorithm[14] but by the usual arguments[7] a sufficiently long random walk is a sample of the square of the wave function.

The convergence of the random walk to the equilibrium distribution was checked several ways. First, it was observed that the various averages, such as the energy and the mean-square displacement reached steady values after about 200 moves/particle. Define Q_n as the probability that a particle will be involved in a permutation cycle of length n. The values of Q_n were kept and it was observed that they were constant irrespective of the starting configuration. Configurations (spatial and permutation) were generated using a small value of C, where long permutations are plentiful,

TABLE IV. Results of the periodic wave function at a density $\rho\sigma^3 = 0.0122$, $\Lambda^* = 0.345$. The values of C are the Fourier components for an fcc crystal $N = 32$ with $A = 21.7$, $B = 0.18$, $D = 0.27$. For the two rows marked with $a*$ the Jastrow parameters were $A = 19.1$, $B = 0.25$, and $D = 1.43$. V_0 is the fraction of vacant Wigner-Seitz cells. It should be noted that $C_{111} > 0$ in order for the particles to be localized on the lattice sites.

C_{111}	C_{200}	C_{220}	C_{311}	C_{222}	V	E	γ	V_0
−0.5	0	0	0	0	9.89	11.64 ± 0.02	0.389	0.150
−1.0	0	0	0	0	9.49	11.73 ± 0.03	0.318	0.089
−2.0	0	0	0	0	8.21	11.88 ± 0.05	0.185	0.004
−1.0	+0.25	0	0	0	9.88	11.92 ± 0.03	0.419	0.190
−1.0	−0.25	0	0	0	8.68	11.88 ± 0.05	0.221	0.030
−1.93	−0.281	+0.095	+0.254	+0.217	8.50	11.72 ± 0.04	0.214	0.006
*−1.93	−0.281	+0.095	+0.254	+0.217	9.69	12.10 ± 0.04	0.236	0.033
*Gaussian with $C = 0.466$					8.80	11.27 ± 0.05	0.213	0.0003

and these configurations were used as a starting point for a random walk at a larger value of C. The population of permutation cycles after equilibrium was established as the same as that from a random walk started from the lattice configuration and the unit permutation. Hence the random walk in permutation space is apparently ergodic; the permutations did not seem to be either frozen in or out.

Finally Green's theorem gives a relationship between two energies which will, in general, only be satisfied if the random walk has sampled enough of configuration space.

$$\langle \nabla^2 W(R) + \vec{\nabla} \ln f(R,P) \cdot \vec{\nabla} W(R) \rangle = 0 \ ,$$

where

$$W(R) = -\ln \left(\psi_T \prod_{i=1}^{N} \phi(\vec{r}_i - \vec{R}_i) \right) \ . \tag{18}$$

Our results show that with 1000 moves/particle the random walk is representative of the full configuration space. Equation (18) is satisfied within the statistical accuracy of our work. This amounts to about 2% of either of the terms in Eq. (18).

Table V contains the energies per particle of the permanent and Gaussian wave functions for $\Lambda^* = 0.345$ and $\rho = 0.0122$ (point B on Fig. 4), for several values of the localization parameter C. The energy of the permanent wave function is higher than that of the Gaussian for all values of C; the kinetic energy of the permanent is slightly smaller since it allows greater excursions from the lattice sites, but the potential energy rises by a larger amount. This can be explained in the following manner: suppose particles i and j have exchanged lattice sites, i.e., $P(i) = j$ and $P(j) = i$. Then both particles i and j will be attracted [see Eq. (14)] to a point at position $\frac{1}{2}(\vec{R}_i + \vec{R}_j)$, and this pseudolattice site will be doubly occupied giving rise to additional potential energy.

The increase in energy of the permanent is quite small for the optimum value of C, because there are very few permutations there. A more sensitive indicator of the effect of the permanent is the population of permutation cycles Q_n, also given in Table V. At the optimum value of $C = 0.265$ the probability of a particle being permuted is only 8×10^{-4}. As C is lowered this number rises very quickly because there is roughly a barrier of $\exp(-2Cr_{nn}^2)$ for the formation of pair permutations. For $C = 0.212$, 7% of the particles are involved in a permutation, for $C = 0.159$, 29% are involved in permutations (one of which had a cycle length of 50).

E. Permanents with vacancies

Instead of allowing exactly one particle per lattice site, a more general type of solid wave function can have a different number of particles and lattice sites. In fact a number of theoretical models have[15] predicted that the ground state of a quantum crystal may have vacancies and if this is the case the solid might have superfluid properties. Table V contains the results of a Monte Carlo calculation with a system of 107 particles and 108 lattice sites. The density is the same, $\rho = 0.0122$, which means the lattice spacing has decreased slightly. The permanent wave function was used, and the permuted lattice sites included the empty one. The energy increased by 0.07 ± 0.01, the increase being split equally between kinetic and potential energies. The above of course is rather a crude test of the concept of vacancies in the ground state, since it is likely that if they do exist in the ground state their concentration is very much smaller than 1%.

The whole question of vacancy formation in these

TABLE V. Variational results for the crystal phase at the density $\rho\sigma^3 = 0.0122$, $\Lambda^* = 0.345$ (point B of the text). The Jastrow parameters are $A = 19$, $B = 0.25$, and $D = 0.25$. The wave function was either a permanent (P), a Gaussian (G), or a permanent with one fewer particle than lattice site (PV). C is the localization parameter of the Gaussian, T and E are the kinetic and total energies in reduced units, γ is Lindemann's ratio, and Q is the probability that a given particle is a member of a permutation cycle of length l.

Wave function	N	Lattice type	C	T	E	γ	Q_1	Q_2	Q_3
P	108	fcc	0.265	2.00	11.28 ± 0.01	0.265	0.9991	7×10^{-4}	1×10^{-4}
P	108	fcc	0.212	1.77	11.44 ± 0.03	0.304	0.93	9×10^{-3}	1×10^{-3}
P	108	fcc	0.159	1.50	11.76 ± 0.03	0.365	0.71	0.04	0.02
G	54	bcc	0.265	2.37	11.19 ± 0.03	0.231	1.0	0.0	0.0
G	108	fcc	0.212	1.99	11.30 ± 0.01	0.285	1.0	0.0	0.0
G	108	fcc	0.159	1.72	11.51 ± 0.01	0.315	1.0	0.0	0.0
PV	107	fcc	0.265	2.05	11.36 ± 0.01	0.265	0.995	0.004	0.001

crystals requires a great deal more careful investigation and considerably more computation. The calculation we have just discussed only tells us that nothing drastic happens when a single vacancy is introduced into the system described by the same wave function as we used in the absence of vacancies.

F. Exact calculations in the solid phase

We used the exact Monte Carlo method sketched above to calculate the ground-state energy and other ground-state properties in the solid phase. Essential to the reliability and efficiency of the exact method is the introduction of a good trial wave function, since this wave function guides the random walk to the important regions of configuration space. We have carried out the exact random walk at three densities near the liquid-solid phase coexistence curve with three types of importance functions: the liquid or Jastrow wave function type, the Jastrow-Gaussian wave function and the periodic wave function. The results for the liquid phase are in Table II, those for the solid phase are in Table VI. Table VI, where comments are made on the agreement of the results obtained with different importance functions.

It might be supposed that one should obtain estimates of the eigenvalue for the ground state using trial wave functions of very different character; for example trial functions describing a liquid or crystal. However, comparison of the "exact" energies computed using different trial functions will only converge to a spatially homogeneous liquid trial function will only converge to a spatially homogeneous distribution and that a walk guided by a solid wave function will only converge to a solidlike state. Of course at any given density there is only one solution to Schrödinger's equation without nodes, but in the thermodynamic limit it seems likely that in the liquid phase, there exists a metastable solid wave function and vice versa. We believe that if a Gaussian wave function is used to guide the random walk, it will converge to a unique metastable solid state (even in the liquid phase), and vice versa with a liquid trial wave function.

The situation with the periodic wave function is somewhat different since particles are free to move throughout the box and can show liquidlike behavior. For this reason it appears that the energy eigenvalue of a random walk guided by this function can converge to either the liquid or solid value, depending on which is lower. The convergence to the liquid value happened for a 32-particle system at a density $\rho = 0.003\,66$ and $\Lambda^* = 0.345$, but not for the 54-particle system where $\Lambda^* = 0.629$ and $\rho = 0.0696$, although the presence of large fluctuations in the random walk indicated to us that it was trying to make the transition to the liquid state. In a larger system such fluctuations become more rare.

We also calculated the exact values of other quantities such as Lindemann's ratio, and the density distribution. The convergence of these quantities is less satisfactory than that of the energy. For example, for the periodic trial function for which the energy converged to the liquid energy, the density distribution still remained nonuniform, although the trend was toward a more uniform distribution. In order to calculate the value of other quantities one needs the weights $\Psi_0(R)/\Psi_T(R)$ and the calculation of these weights is subject to large fluctuations. In fact one can only trust these weights if one has other reasons for believing that the ground state resembles the trial wave function.

TABLE VI. Results of the exact Monte Carlo simulation at three densities with different trial functions for the crystal phase. The symbols *A*, *B*, *C*, and *D* are the same as in Table II. The entries in the last column show the kind of wave function used for *importance sampling* in the exact Monte Carlo simulation. For the points *B* and *C*, the different *importance functions* lead to energies which agree within the rather small statistical errors. The results for point *A* do not agree so well—probably due to difficulties in convergence in one of the runs. The basic idea of importance functions and importance sampling is discussed in the text immediately after Eq. (5).

$\rho\sigma^3$	Λ^*	N	A	B	C	D	T_M	E_0	Point	Importance function
0.003 66	0.345	32	17.6	0.28	0.12	0.18	0.63	1.56 ± 0.01	*A*	Jastrow-Gaussian
0.003 66	0.345	32	22.4	0.19	0.12	0.18	0.47	1.51 ± 0.01	*A*	Jastrow-Periodic
0.012 2	0.345	54	19.2	0.25	0.23	0.24	1.95	11.09 ± 0.01	*B*	Jastrow-Gaussian
0.012 2	0.345	54	19.2	0.25	0.35	0.24	2.20	11.07 ± 0.01	*B*	Jastrow-Gaussian
0.012 2	0.345	54	21.6	0.19	0.78	0.24	2.40	11.07 ± 0.02	*B*	Jastrow-Periodic
0.069 6	0.629	54	9.0	1.0	1.0	0.29	4.79	48.76 ± 0.05	*C*	Jastrow-Gaussian
0.069,6	0.629	54	10.4	0.78	1.95	0.32	4.23	49.1 ± 0.2	*C*	Jastrow-Periodic

V. EXACT LIQUID-SOLID PHASE COEXISTENCE

The phase boundary estimated from our exact energies is shown with the solid curve in Fig. 4. As before the curve satisfies the equation $C^*\rho^{-2/3} = 14.8$. Since we have only done exact calculations at three points this curve is a rough estimate of the actual curve. Note that this curve predicts that the one component plasma will crystallize at $r_s = 130 \pm 10$. This is in good agreement with the recent value $r_s = 135$, obtained by Glyde *et al.*[16]

The comparison of the variational and exact coexistence curves shows what we believe to be a general feature of variational calculations: A variational study of liquid and solid phases will always favor the solid phase; the variational solid energy is closer to the exact energy than is the liquid variational energy to the exact energy. In other words, the Gaussian-Jastrow wave function is a better approximation to the solid phase than is the Jastrow wave function to the liquid phase.

VI. LINDEMANN'S RATIO AND THE LOCAL DENSITY DISTRIBUTION

We have tabulated Lindemann's ratio γ for the various trial wave functions discussed above. The variational results in Table III indicate that the solid is unstable if γ is greater than 0.28 ± 0.02. There is considerable uncertainty in this number because of the limitations of the variational method. A similar value has been obtained at the melting density[12] of He^4. This is rather surprising considering the difference in potential and possibly in the mechanism behind the solidification.

Using the weights from the exact method we have determined the ground-state density distribution in the solid at $\Lambda^* = 0.345$ and $\rho = 0.0122$. Shown in Fig. 5 is the sphericalized distribution about a lattice site; the solid curve is a Gaussian with the same moment as the exact points. Table VII contains the Fourier components of the exact density distribution, at this density, where

$$\rho_{\vec{k}} = (1/N)\left\langle \sum_{i=1} \exp(i\vec{k}\cdot\vec{r}_i)\right\rangle \quad . \tag{19}$$

Also shown are the Fourier components of a Gaussian fitted to the second moment. Within the errors of our calculation it appears that the density distribution is closely approximated by a Gaussian. It should be noted however that this Gaussian is appreciably narrower than the Gaussian in the trial wave function. This feature of the trial function was first noted by Hansen and Levesque.[12]

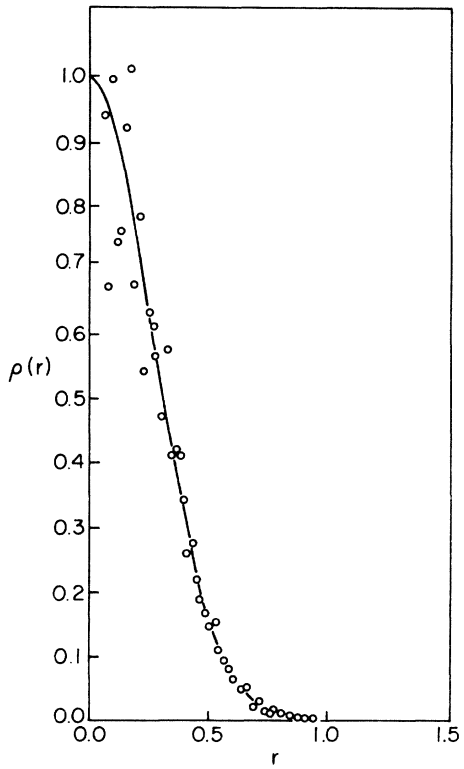

FIG. 5. Single-particle density around a lattice site in the solid, $\rho = 0.0122$ and $\Lambda^* = 0.345$ (point B on Fig. 4). The circles are the result of an exact calculation, the curve is a Gaussian fitted to the mean-square value of r; r is in reduced units, $\rho(r)$ in arbitrary units.

VII. UPPER BOUND TO THE SUPERFLUID FRACTION

Recently it has been conjectured[17] that He^4 has a small and as yet undetected nonzero superfluid component. One can easily get an upperbound to the superfluid fraction by a variational approach. Using the same method suggested by Saslow,[18]

TABLE VII. Fourier components of the single-particle density evaluated exactly (ρ_E) and as predicted from a Gaussian distribution (ρ_G). The second moment of the Gaussian gives a Lindemann's ratio of $\gamma = 0.244$.

$\vec{k}$	$\rho_E(\vec{k})$	$\rho_G(\vec{k})$
000	1.0	1.0
110	0.552	0.556
200	0.311	0.310
112	0.169	0.172
022	0.093	0.0954
013	0.050	0.0533
222	0.027	0.0298
123	0.011	0.0166
004	−0.0009	0.00915
033	0.0011	0.00513
114	−0.0025	0.00513

we have used our exact density distribution results to determine this upper bound to the superfluid fraction at a density $\rho = 0.0122$ and $\Lambda^* = 0.345$ for the Yukawa crystal. An upper bound to the superfluid fraction ρ_s is given by

$$\rho_s \lesssim \sum_{\vec{k}} \phi_{\vec{k}} \vec{k} \cdot \left(2\rho_{\vec{k}} \vec{V}_0 / |\vec{V}_0| + \sum_{\vec{k}} \vec{k}' \rho_{\vec{k}-\vec{k}'} \phi_{\vec{k}'} \right) , \tag{20}$$

where $\vec{k}$ is a wave vector in the reciprocal lattice, ρ_k is the exact[19] fourier component of the density, as given in Table VII and V_0 is the flow field velocity. The ϕ_k are parameters which are varied to minimize the upper bound. This minimization yields a set of linear equations which are easily solved numerically once the exact ρ_k are known.[20] For a crystal with the values of ρ_k in Table VII (and others at higher values of k) this method yields $\rho_s < 0.13$. This upper bound, Eq. (20), can be used with any model wave function for a crystal. Care should be taken in its application. There are some model wave functions for which it is extremely plausible that ρ_s is zero e.g., a model with strictly localized particles on lattice sites would rule out *any flow* of any kind. For our wave functions the ρ_k's are all rather similar and we do not see any reason why *some* flow could not take place. Whether it would be superflow is yet another matter.

This value is in reasonable agreement with the upper bounds as calculated by Saslow[18] for solid He.[4] In fact the upper bound is almost entirely a function of the mean-square displacement from a lattice site given that the density distribution is well approximated by a Gaussian function. Since no component of that magnitude has been observed in solid He^4, it can be concluded that this method does not yield a very good estimate of the superfluid fraction.

VIII. CONCLUSION

A system of particles interacting with a Yukawa potential is an example of a system with a potential which is both short range and soft. At high density it behaves like a Coulomb system. Only if the kinetic energy is small enough will it crystalize. Our exact Monte Carlo calculations imply that this will happen only if $\Lambda^* < 0.48$. The energies of the liquid and solid phases are extremely close to each other over a large density range; the relative width of the coexistence region is estimated to be only 1%. This emphasizes the importance of doing accurate calculations to find the phase boundaries for such smooth potentials.

We have found that our variational calculations tend to favor the solid phase. That is our solid-phase variational calculations are in closer agreement with the exact Monte Carlo results than the variational results we obtained for the liquid phase. While this conclusion is of course only strictly true for the class of variational wave function we have used we believe it to be rather generally valid. The reason for this belief is that the configuration space of the crystalline phase is considerably simpler than that of the fluid phase. The particles are localized and do not move freely past one another. Hence it is easier to build a variational wave function for the crystal phase as compared with the fluid phase. Both functions contain two-particle correlations, the function for the crystal phase contains single-particle correlation in addition.

The Yukawa crystal is in many ways similar to solid helium. It will melt if Lindemann's ratio is greater than about 0.28. The single-particle density is well approximated by a Gaussian distribution. A periodic trial wave function has a significantly higher energy than the Gaussian trial wave function, probably because it allows double occupancy of lattice sites. We have found that it is possible to sample a symmetrized Gaussian wave function and that its variational energy is slightly higher than that of the unsymmetrized Gaussian. Adding one vacancy to this crystal increases the energy. However, it is difficult within the variational approach to determine whether the ground-state crystal contains any vacancies. We have also determined that the superfluid fraction in the crystal is less than 0.13. As we have already mentioned earlier this bound seems rather insensitive to the form of the variational function, or whether we use results from variational calculations or our exact simulations. They all produce very similar values for the Fourier components $\rho_{\vec{k}}$ of the density, on which the bound depends.

†Supported by the Department of Energy under Contract No. EY-76-C-02-3077*000 and by Grant No. DRM-74-23494 with the NSF and in part by the NSF through the Materials Science Center, Cornell University, under Grant No. DMR-72-03029.

[1] J. P. Valleau and G. P. Torrie, in *Modern Theoretical Chemistry*, edited by B. Berne (Plenum, New York, 1976), Chap. 5.

[2] D. Ceperley, M. H. Kalos and G. V. Chester, Phys. Rev. D 13, 3208 (1976).

[3]The "Bethe" potential to which we refer is also commonly know as the "homework" potential.
[4]S. G. Cochran, Ph.D. thesis (Cornell University, 1974) (unpublished).
[5]D. Ceperley, G. V. Chester, and M. H. Kalos (unpublished).
[6]F. A. Lindemann, Z. Phys. 11, 609 (1910).
[7]N. Metropolis, A. Rosenbluth, M. Rosenbluth, A. Teller, and E. Teller, J. Chem. Phys. 27, 1207 (1957).
[8]W. McMillan, Phys. Rev. 138, A422 (1965).
[9]M. H. Kalos, D. Levesque and L. Verlet, Phys. Rev. A 9, 2178 (1974).
[10]M. H. Kalos, Phys.Rev. A 2, 250 (1970).
[11]K. S. Liu, M. H. Kalos, and G. V. Chester, Phys. Rev. A 10, 303 (1974).
[12]J. P. Hansen and D. Levesque, Phys. Rev. 165, 293 (1968).
[13]D. N. Lowy and C. W. Woo, Phys. Lett. 56A, 402 (1976); D. N. Lowy and C. W. Woo, Phys. Rev. B 13, 3790 (1976).
[14]It is clearly not necessary to try to permute particles afar apart since those moves will be rejected. However, with the present method less time was spent in computing the probabilities of these permutations than in calculating the distances for Ψ_T. Hence it does not seem worth the trouble to improve it. The choice of a pair transition move is appropriate, since pair permutations are more numerous than more complicated permutations.
[15]A. F. Andreev and I. M. Lifshitz, Sov. Phys.-JETP 29, 1107 (1969). G. V. Chester, Phys. Rev. A 2, 256 (1970).
[16]H. R. Glyde, G. H. Keech, R. Mazaghi and J. P. Hansen, Phys. Lett. 58A, 2226 (1976).
[17]A. J. Leggett, Phys. Rev. Lett. 25, 1543 (1970); V. Chui, Cornell University Ph.D. thesis, 1970 (unpublished); A. Widom, J. Low. Temp. Phys. 23, 335 (1976); Y. C. Cheng, Phys. Rev. B 14, 1946 (1976).
[18]W. M. Saslow, Phys. Rev. Lett. 36, 1151 (1976).
[19]Unless the exact ground-state values of ρ_k are used this method will not give a rigorous upper bound.
[20]In practice one can only use a finite number of k vectors. We chose $|k| < 6$. Symmetry reduces the number of independent equations considerably.